Williamsburg, Virginia
ACTIVE 04
2004 September 20-22

A New Approach to Identify Optimal Properties of Shunting Elements for Maximum Damping of Structural Vibration Using Piezoelectric Patches

Junhong Park[1], Daniel L. Palumbo[2],
National Research Council[1], Structural Acoustics Branch[2], NASA Langley Research Center,
Hampton, VA 23681-2199,
junhongpark@hotmail.com

ABSTRACT

The use of shunted piezoelectric patches in reducing vibration and sound radiation of structures has several advantages over passive viscoelastic elements, e.g., lower weight with increased controllability. The performance of the piezoelectric patches depends on the shunting electronics that are designed to dissipate vibration energy through a resistive element. In past efforts most of the proposed tuning methods were based on modal properties of the structure. In these cases, the tuning applies only to one mode of interest and maximum tuning is limited to invariant points when based on den Hartog's invariant points concept. In this study, a design method based on the wave propagation approach is proposed. Optimal tuning is investigated depending on the dynamic and geometric properties that include effects from boundary conditions and position of the shunted piezoelectric patch relative to the structure. Active filters are proposed as shunting electronics to implement the tuning criteria. The developed tuning methods resulted in superior capabilities in minimizing structural vibration and noise radiation compared to other tuning methods. The tuned circuits are relatively insensitive to changes in modal properties and boundary conditions, and can applied to frequency ranges in which multiple modes have effects.

1. INTRODUCTION

As advanced structural elements such as honeycomb panels are increasingly used in vehicles, total mass of the structure continues to decrease, especially in aerospace applications [1]. The decrease in airframe mass can result in increased cabin noise. To maintain interior noise levels, either existing treatment must be supplemented (adding mass) or more efficient treatment must be developed. Structural vibration damping contributes to the minimization of noise-related problems. To increase structural damping and to minimize noise generation, it is common practice to apply viscoelastic materials to the structures, or to add acoustic treatments [2,3]. Recently, more active methods utilizing smart components and electro-mechanical couplings have been proposed [4] and have been used in the control of aircraft interior noise. Control actuators often proposed in such systems are piezoelectric patches, shape memory alloys, and fluidic actuators. Among them the piezoelectric patches has been most widely used in structural acoustic control. Active control systems using feedback or feed forward control techniques require supporting electronics that typically consist of a digital signal processor system and components for sensing and actuating imbedded elements. By utilizing passive shunting techniques as shown in Figure 1 the required hardware can be significantly reduced with increased robustness.

The use of shunted piezoelectric patches to control structural vibration was first proposed by Forward [5] to stabilize optical systems. Hagood and Flotow [6] presented a more complete analysis of the shunted damping of structures. Effects from the electronic network were analyzed and incorporated in the variation of the elastic properties of the patch. The performance of the piezoelectric patches in reducing the vibration response was significantly related to the characteristics of shunting electrical circuits. The tuning of the values of the electronic components was performed based on the shunt circuit's effect on the structure's modal response. Resonant shunt circuits were optimized using den Hartog's invariant point concept and the pole placement technique. Many approaches have been proposed to optimally tune the shunting electrical networks [7-10]. In addition to *RL* resonant circuits, various *RLC* circuits have been proposed [11-15]. One review of these methods can be found in the reference [16]. However, most of the tuning methods are based on the modal properties of the structure when treated with piezoelectric patches. Consequently, the tuning applies only to a limited number of modes at natural frequencies. Also, the tuning of individual circuits, each attached to one of multiple piezoelectric patches, can be complicated due to interaction between patches through the structure. Difficulty also arises when the circuit's

bandwidth covers a frequency range in which intermodal couplings are not negligibly small due to high modal density within the band.

In this study, the optimization of the shunting electrical networks is performed based on the wave propagation characteristics of the structure and wave transmission characteristics through the piezoelectric patches. The shunting electrical networks influences the dynamic mechanical properties of the patch. Although many approaches have been proposed to separate the physical degrees of freedom between the modal properties and electrical charge, combining the effects of the electrical circuit to the dynamic mechanical properties and deleting the physical degrees of freedom related to electrical charge yield the same results since the physical quantities related to mechanical and electrical variables are uncoupled in the system equations when external excitation is not applied to the electrical circuit. The energy dissipated as the propagating structural waves transmit and are reflected from the piezoelectric patch is calculated. The optimal tuning is obtained to maximize this structural energy dissipation. The effects of location of piezoelectric patches on and boundary conditions of the structure are investigated. The performance of the tuning criteria is confirmed through calculating the forced vibration of the beam and is compared to a conventional method based on den Hartog's invariant point concept. An active filter technique to implement the optimal shunting criteria is proposed.

2. EFFECTS OF SHUNTING NETWORKS

When the piezoelectric patch is shunted as shown in Figure 1, the patch acts as a vibration absorber. In this case, the effects of shunts on the piezoelectric materials can be analyzed using linear constitutive equation [17] as

$$\begin{bmatrix} D_3 \\ S_{11} \end{bmatrix} = \begin{bmatrix} \varepsilon_3^T & d_{31} \\ d_{31} & s_{11}^E \end{bmatrix} \begin{bmatrix} E_3 \\ T_{11} \end{bmatrix} \tag{1}$$

where D_3 is the electrical displacement, S_{11} is the strain, E_3 is the electrical field, T_{11} is the stress, d_{31} is the piezoelectric constant, s_{11}^E is compliance at constant electrical field, and ε_3^T is the electrical permeability at constant stress. The dynamic displacement of the patch is coupled to electrical charges through the piezoelectric effects represented by the coefficients, d_{31}. The voltage (V) and current (I) are related to electrical variables as $V = \int_0^{t_p} E_3 dz$ and $I = \int_A D_3 dA$ where t_p is the thickness and A is the area of the patch. By taking the Laplace transform of the above relationships after assuming uniform spatial distribution of the electrical field and electrical displacement of piezoelectric patch, equation (1) is converted to a more convenient definition to derive admittance of shunting networks as [6]

$$\begin{bmatrix} I \\ S_{11} \end{bmatrix} = \begin{bmatrix} sC_p^T & sAd_{31} \\ d_{31}/t_p & s_{11}^E \end{bmatrix} \begin{bmatrix} V \\ T_{11} \end{bmatrix} \tag{2}$$

where C_p^T is the inherent capacitance of the patch and s is the Laplace parameter. In this case, shunting of the patch has primary impacts on the dynamic stiffness of the patch. When the external electrical source to the piezoelectric patch is not present (I=0), the effects of electrical network on the elastic moduli of the shunted patch can be simplified as

$$E_p^{SU} = \frac{E_p^E \left(sC_p^T + Y^{SU} \right)}{\left(sC_p^T + Y^{SU} \right) - k_{31}^2 sC_p^T}, \tag{3}$$

where E_p^E ($=1/s_{11}^E$) is the elastic moduli of the patch at short circuit, Y^{SU} is the electrical admittance of the shunting networks, and k_{31} is the electromechanical coupling coefficient for transverse operation ($= d_{31}/\sqrt{s_{11}^E \varepsilon_3^T}$) [6]. From equation (3) variation of the complex moduli of the patch with the admittance of electrical circuit is obtained after substituting s=iω where i $=\sqrt{-1}$. When the usual complex notation is used, $w(x,t) = \mathrm{Re}\{\hat{w}(x)e^{i\omega t}\}$ for w the displacement, complex moduli are defined as,

$$\hat{E}_p^{SU} = E_{p,d}^{SU}(\omega) + \mathrm{i}E_{p,l}^{SU}(\omega) = E_{p,d}^{SU}(\omega)\left[1 + i\eta_P^{SU}(\omega)\right], \tag{4}$$

where $E_{p,d}^{SU}$ is the dynamic moduli, $E_{p,l}^{SU}$ is the loss moduli, and η_P^{SU} is the loss factor. Arbitrary electrical circuits composed of multiple resistors, capacitances, and inductances in series or in parallel can be considered. The bending stiffness of the beam treated by the patch is given as

$$\hat{D}_{x1} = \hat{E}_b J_b + \hat{E}_p^{SU} J_p = D_{x1}\left(1 + \mathrm{i}\eta_D^{SU}\right), \tag{5}$$

where $\hat{E}_b$ is the complex moduli of the beam material, J_b and J_p are the moments of inertia of the beam and the patch, respectively. The bending stiffness of the beam itself is given as $\hat{D}_{x2} = \hat{E}_b J_b$.

The variation of the complex modulus, $\hat{E}_p^{SU}$ and the bending stiffness, $\hat{D}_{x1}$, with respect to the admittance, Y^{SU}, is most significant near the values which make the imaginary part of the denominator in equation (3) close to zero, the resonance condition of the *RLC* circuit. Consequently, its variation is limited when the shunt is consisted only of resistive elements. Only when the shunting circuit is composed both of reactive and resistive elements, wide variation of the resulting complex modulus is possible. The dynamic modulus of the shunted patch can be negative or positive. From the wide variation of the dynamic modulus and loss factor, an arbitrary value of the dynamic bending stiffness, $\hat{D}_{x1}$, is obtained. The condition of maximum loss factor or maximum loss moduli of the bending stiffness does not result in minimum structural vibration response. Instead, the values that minimize the vibration and sound generation of structures and maximize the vibration energy dissipation at the patch are desired in noise control applications. To achieve this goal, the forced vibration and resulting sound generation of the beam may be considered, which require estimation of variation of the modal properties depending on the shunting networks. In this study, wave propagation characteristic of structural waves through piezoelectric patch is investigated to obtain optimal shunting properties without requiring calculation of the modal properties.

3. WAVE PROPAGATION NEAR THE PIEZOELECTRIC PATCHES

To analyze reflection, transmission, and dissipation of the wave propagating near the piezoelectric patch, wave propagations as shown in Figure 2 for different boundary conditions were considered. The edge of the beam in Figures 2(a) and (b) at x=-L and x=-(L+L_e), respectively, can be supported by geometric or general boundary conditions. The beam was assumed to be infinitely long in the x-direction in order to allow for the calculation of the reflection ratio of the normally incident bending waves as assumed in calculating reflection ratios at viscoelastically supported edges [18]. The equation of motion for the free transverse vibrations (when effects of shear deformation and rotary inertia are neglected) is,

$$D_x \frac{\partial^4 w}{\partial x^4} + M \frac{\partial^2 w}{\partial t^2} = 0, \tag{6}$$

where D_x is the bending stiffness, w is the transverse displacement, and M is the mass per unit length. To calculate the wave propagation characteristics at the edge, normally incident harmonic bending waves with complex amplitude $\hat{C}_{22}$ were assumed to propagate toward the patch from $x = \infty$. The reflection, transmission and dissipation of the incident vibration energy are calculated by obtaining the resultant wave propagation induced by this disturbance near the patch. The calculation depends on various boundary conditions, for example the different cases as shown in Figure 2.

When the piezoelectric patch is attached to the edge of the beam shown in Figure 2(a) the beam transverse displacement is given as

$$\hat{w}(x) = \left(\hat{C}_{11}e^{-ik_1(x+L)} + \hat{C}_{12}e^{ik_1x} + \hat{C}_{13}e^{-k_1(x+L)} + \hat{C}_{14}e^{k_1x}\right)(1-H(x)) + \left(\hat{C}_{21}e^{-ik_2x} + \hat{C}_{22}e^{ik_2x} + \hat{C}_{23}e^{-k_2x}\right)H(x) = w_1(x)(1-H(x)) + w_2(x)H(x) \tag{7}$$

where H is the Heavyside step function, k_1 and k_2 are the wavenumbers related to the circular frequency as $k_{1,2} = \left(\omega^2 M_{1,2} / D_{x1,2}\right)^{1/4}$. A continuous neutral surface of zero bending stiffness through the discontinuities at x=0 is assumed. By attaching the patch symmetrically with respect to the neutral surface of the beam, this assumption can be satisfied. By applying the boundary conditions of the beam, the complex coefficients ($\hat{C}_{11}$-$\hat{C}_{14}$, $\hat{C}_{21}$, $\hat{C}_{23}$) in equation (7) are determined. Note that there are six unknowns with $\hat{C}_{22}$ an input variable. The boundary conditions are

- at x=0

$$\hat{w}_1(0) - \hat{w}_2(0) = 0, \ \frac{\partial \hat{w}_1}{\partial x}(0) - \frac{\partial \hat{w}_2}{\partial x}(0) = 0, \tag{8a,b}$$

$$\hat{D}_{x1}\frac{\partial^3 \hat{w}_1}{\partial x^3}(0) - \hat{D}_{x2}\frac{\partial^3 \hat{w}_2}{\partial x^3}(0) = 0, \ \hat{D}_{x1}\frac{\partial^2 \hat{w}_1}{\partial x^2}(0) - \hat{D}_{x2}\frac{\partial^2 \hat{w}_2}{\partial x^2}(0) = 0, \tag{8c,d}$$

- at x=-L (for different geometric boundary conditions)

$$\hat{w}_1(-L) = 0, \ \frac{\partial \hat{w}_1}{\partial x}(-L) = 0, \text{ (for clamped edge)} \tag{8e,f}$$

$$\frac{\partial^2 \hat{w}_1(-L)}{\partial x^2} = 0, \ \frac{\partial^3 \hat{w}_1(-L)}{\partial x^3} = 0, \text{ (for free edge)} \tag{8g,h}$$

$$\hat{w}_1(-L)=0,\ \frac{\partial^2\hat{w}_1(-L)}{\partial x^2}=0\text{. (for simply-supported edge)} \qquad (8i,j)$$

After replacing equation (7) into six boundary conditions in equation (8), the unknown coefficients are obtained. Consequently, the response of the beam to external excitation of the incident bending waves of complex magnitude $\hat{C}_{22}$ is calculated. The same numerical procedures are repeated for the piezoelectric patches attached to different location of the beam. The differences are on the number of boundary conditions and the assumed beam displacement functions. The beam displacements are given as

- when separated from edge (Figure 2(b))

$$\begin{aligned}\hat{w}(x)=&\left(\hat{C}_{11}e^{-ik_1(x+L)}+\hat{C}_{12}e^{ik_1x}+\hat{C}_{13}e^{-k_1(x+L)}+\hat{C}_{14}e^{k_1x}\right)\left(H(x+L)-H(x)\right)+\left(\hat{C}_{21}e^{-ik_2x}+\hat{C}_{22}e^{ik_2x}+\hat{C}_{23}e^{-k_2x}\right)H(x)\\&+\left(\hat{C}_{31}e^{-ik_1(x+L+L_e)}+\hat{C}_{32}e^{ik_1(x+L)}+\hat{C}_{33}e^{-k_1(x+L+L_e)}+\hat{C}_{34}e^{k_1(x+L)}\right)\left(1-H(x+L)\right)\end{aligned}, \qquad (9a)$$

- when far from edges (Figure 2(c))

$$\begin{aligned}\hat{w}(x)=&\left(\hat{C}_{11}e^{-ik_1(x+L)}+\hat{C}_{12}e^{ik_1x}+\hat{C}_{13}e^{-k_1(x+L)}+\hat{C}_{14}e^{k_1x}\right)\left(H(x+L)-H(x)\right)+\left(\hat{C}_{21}e^{-ik_2x}+\hat{C}_{22}e^{ik_2x}+\hat{C}_{23}e^{-k_2x}\right)H(x)\\&+\left(\hat{C}_{32}e^{ik_1(x+L)}+\hat{C}_{34}e^{k_1(x+L)}\right)\left(1-H(x+L)\right)\end{aligned}. \qquad (9b)$$

Boundary conditions are defined in the exactly same way as shown in equation (8). The calculation can be performed with and without taking into account material damping of the structure. When the patch is applied to conventional metal structures, the damping in the structure itself is negligibly small in general. In such cases, the dissipation of the vibrational energy through the piezoelectric patches is calculated as

$$Disspation(\%)=\begin{cases}\left(1-\left|\hat{C}_{21}\right|^2\Big/\left|\hat{C}_{22}\right|^2\right)\times 100 & \text{(for the patch attached near an edge, Figure 2 (a) and (b))}\\ \left(1-\left(\left|\hat{C}_{21}\right|^2+\left|\hat{C}_{32}\right|^2\right)\Big/\left|\hat{C}_{22}\right|^2\right)\times 100 & \text{(for the patch far from the edges, Figure 2 (c))}\end{cases}. \qquad (10)$$

Maximum dissipation of the vibrational energy is directly related to minimization of the forced vibration and sound radiation as illustrated for the case of a plate supported by viscoelastic elements [18]. Wave propagation characteristics are derived by calculating the effects of the shunting electrical networks on the bending stiffness of the beam. From these results, the optimal shunting network that maximizes the dissipation in equation (10) is obtained numerically without requiring calculation of the modal properties.

4. BEAM VIBRATION CALCULATION

The performance of the piezoelectric patches in reducing the vibration of structures is estimated through calculating the forced vibration of a beam of finite size from which tuning efficiency is predicted. Figure 3 shows the beam supported by general boundary conditions and controlled by piezoelectric patch. By modifying the stiffness of the springs supporting the beam, the vibration characteristic of the beam of arbitrary edge conditions is analyzed [19, 20]. The kinetic, T_K, and potential energy, V_P, for transverse vibration of the beam is calculated using:

$$T_K=\int_{-a}^{a}\frac{1}{2}M_b\left(\frac{\partial w}{\partial t}\right)^2dydx+\int_{x_1}^{x_2}\frac{1}{2}\left(M_p-M_b\right)\left(\frac{\partial w}{\partial t}\right)^2dydx, \qquad (11a)$$

$$V_P=\int_{-a}^{a}\frac{1}{2}D_b\left(\frac{\partial^2 w}{\partial x^2}\right)^2dx+\int_{x_1}^{x_2}\frac{1}{2}\left(D_p-D_b\right)\left(\frac{\partial^2 w}{\partial x^2}\right)^2dx+\frac{1}{2}s_{t1}w(-a)^2+\frac{1}{2}s_{r1}\left(\frac{\partial w(-a)}{\partial x}\right)^2+\frac{1}{2}s_{t2}w\left(\frac{a}{2}\right)^2+\frac{1}{2}s_{r1}\left(\frac{\partial w(a)}{\partial x}\right)^2, \qquad (11b)$$

$$W_F=\int_{-a}^{a}\frac{1}{2}f(x,t)w(x,t)dx\,. \qquad (11c)$$

In the Rayleigh-Ritz method, the transverse displacement of the beam is approximated as

$$w(x,t)=\sum_{m=1}^{N}\phi_m(x)\alpha_m(t), \qquad (12)$$

where ϕ_m are the trial functions chosen from a complete set, and α_m are the generalized coordinates. After substituting equation (12) into equation (11), Lagrange's equations of motion,

$$\frac{d}{dt}\left(\frac{\partial L_S}{\partial\dot{\alpha}_m}\right)-\frac{\partial L_S}{\partial\alpha_m}=0,\qquad m=1,2,...,N, \qquad (13)$$

are applied, where $L_S = T_K - V_P + W_F$ is the system Lagrangian. This yields a set of equations of motion

$$[M]\{\ddot{\alpha}\}+\left[K^e+K^V\right]\{\alpha\}=\{f\}, \qquad (14)$$

where $[M]$, $[K^e]$, and $[K^V]$ are the mass and stiffness (from springs at edges and beam strain energies) matrices , respectively. When the harmonic excitation of the beam is considered with time dependence of $e^{-i\omega t}$, the equations of motion are

$$-\omega^2[M]\{\ddot{\alpha}\}+[K^e+K^V]\{\alpha\}=\{f\}. \tag{15}$$

The polynomial functions are used as trial functions as

$$\phi_m(x)=x^m, m=0,N\ . \tag{16}$$

Consequently, the mass and stiffness matrices are calculated as

$$[M_{mp}]=\frac{M_b}{m+p+1}\left(a^{m+p+1}-(-a)^{m+p+1}\right)+\frac{(M_p-M_b)}{m+p+1}\left(x_2^{m+p+1}-x_1^{m+p+1}\right), \tag{17a}$$

$$[K^V_{mp}]=\begin{cases}0, m<2 \quad \text{or} \quad p<2\\ \dfrac{D_b m(m-1)p(p-1)}{m+p-3}\left(a^{m+p-3}-(-a)^{m+p-3}\right)+\dfrac{(D_p-D_b)m(m-1)p(p-1)}{m+p-3}\left(x_2^{m+p-3}-x_1^{m+p-3}\right) otherwise\end{cases}, \tag{17b}$$

$$[K^e_{mp}]=\begin{cases}s_{t1}(-a)^m(-a)^p+s_{t2}a^m a^p, m=0 \quad \text{or} \quad p=0\\ s_{t1}(-a)^m(-a)^p+s_{t2}a^m a^p+s_{r1}mp(-a)^{m-1}(-a)^{p-1}+s_{r2}mpa^{m-1}a^{p-1}, otherwise\end{cases}, \tag{17c}$$

$$[f_m]=\int_{-a}^{a} f(x,t)\phi_m(x)dx\cdot \tag{17d}$$

5. RESULTS AND DISCUSSIONS

If the shunting elements are not present in Figure 1, there is no energy loss in the system when the material damping is small. Appreciable damping occurs only when electrical energy produced through piezoelectric effects is dissipated into the electrical network. The patch with resistive shunting element acts as a control device of the system to absorb and dissipate vibration energy and to minimize undesirable vibration of the structure and noise generation especially when the external excitation has a broadband characteristic. Two different shunting networks (resistive and resonant) are considered. To compare results with previously published data, a beam structure and a piezoelectric patch of similar dimensions and material properties to those in the previous publication [6] are used in this study. (L = 6.2 cm, a = 14.65 cm, t = 3.17 mm, E_b^E =73 GPa, E_p^E = 63 GPa, C_p^S=0.156 μf, ε_e^T =1700 ε^o, k_{31} = 0.35, d_{31} = 180e-12 m/v).

A. Resistive shunting

When the shunting network consists only of a resistor, the resistor increases the material damping of the piezoelectric patches by dissipating converted electrical energy into heat. Using the wave propagation approach, the amount of energy dissipation is calculated as presented in section 2. Figure 4 shows the energy dissipation on patches attached to different locations of the beam at the fundamental frequency. Figure 4 (a) shows the variation with separation distance from the clamped edge of the beam. The maximum dissipation occurs when the patch is attached to the clamped edge of the beam. With increasing separation distance, the energy dissipation is decreased. The maximum dissipation occurred at approximately the same resistance values regardless of the position of the patch relative to the edge. Obviously, the optimal position of the patch to maximize its performance to induce maximum energy dissipation is near the clamped edge. Figure 4 (b) shows the comparison for the patch attached to edge of the beam with different boundary conditions – clamped, free, simply-supported (Figure 2 (a)), and far from both edges (Figure 2 (c)). The maximum amount of energy dissipation occurred when the edge is clamped. For other boundary conditions, the energy dissipation was smaller. The energy dissipation was negligibly small when the patch is attached to the free edge.

Figure 5 shows the variation of the energy dissipation with frequency and resistance when the patch is attached to the beam's edge (Figure 1(a)). For each frequency, there is one maximum in the amount of the energy dissipation. When the patch is attached to the free edge (Figure 5(b)), non-negligible energy dissipation occurs only at high frequencies where the length of the patch is comparable to the excitation wavelength (λ=10 cm at f=2 kHz). Figure 6 shows optimal resistance values taken from Figure 5 at the point of maximum energy dissipation. The optimal values are relatively insensitive to boundary conditions, and are very similar to the values that induce maximum material damping of the patch and the maximum modal damping of the beam [6].

For the structure and patch considered in this study, the amount of energy dissipation obtained using purely resistive shunting is generally less than 5 %. This amount of damping does not justify the added cost and

complexity when compared to passive techniques [18]. To increase the dissipation, the current flowing through the resistor must be amplified. This is accomplished with resonant shunting circuits.

B. Resonant shunting

When a resonant shunting element is used, the condition of the maximum dissipation is very sensitive to circuit parameters. Optimization of the resonant network is not as straight forward as the resistive network. Until now many optimization techniques have been proposed. When the resonant shunting is used, the resonance due to the capacitance of the patch and the inductance of the shunting network significantly increases the current flowing through the resistance and consequently increases the energy dissipation and damping capabilities of the patch. To investigate these effects, the *RLC* circuit shown in Figure 1 is considered. Other configurations, such as *RLC* in parallel as discussed in several other publications, are also possible.

Figure 7 shows the variation of the vibration energy dissipation with R and L when C=0 at fundamental frequency of the beam (f=33.5 Hz). L_{res} is the resonant inductance value, $\left(\omega^2 C_p^S\right)^{-1}$. The calculation was repeated for different boundary conditions of the beam. In the simulation results, the performance of the patch in dissipating the vibration energy when the boundary condition is clamped is better than that of any other boundary conditions. When the boundary condition is clamped or infinite, there are values of R and L that induces completely dissipation of the incident vibrational energy near $R\approx300\ \Omega$ and L=0.97 L_{res} at fundamental frequency. This condition corresponds to the values that lead the dynamic stiffness, $\hat{D}_{x1}$, to be negative and the loss factor to be positive. As the resistance and inductance values deviate from the optimal value, the amount of vibrational energy dissipation starts to decrease very rapidly. Dissipation is more sensitive to the inductance value. The optimal inductance value is smaller than the resonant inductance by 1-2 %.

In Figure 7(a) and (d), there are another values of R and L than induces complete dissipation of the incident vibrational energy near $R\approx5\ \Omega$ and L=0.96 L_{res}. This condition results in positive dynamic moduli and loss factor of $\hat{D}_{x1}$. However, the occurrence of this optimal value is extremely sensitive to the inductance values, L, and requires very small value of R which may not easy to implement using conventional *RLC* circuit in actual situations especially when the required inductance value is large. In the following studies, this condition was not considered and only the optimal values that induce complete vibration energy dissipation with negative dynamic moduli of $\hat{D}_{x1}$ was selected as the optimal values.

Figure 8 shows the variation of these optimal inductance and resistance with frequency. The values obtained from the den Hartog's invariant point concept are plotted also. The optimal values are similar to each other, but considerable difference exists in the values of the resistance. To implement the condition calculated in Figure 8, frequency dependent variation of the resistance and inductance is required. To satisfy this condition, it is more straightforward to consider frequency-dependent admittance values. Figure 9 shows the admittance of the electrical circuit that results in complete absorption of the incident vibrational energy. The variation of the admittances when the shunting elements are composed of constant values of R and L is also plotted. The optimal value of R and L was taken as the value that completely absorbs the vibration energy at the first resonance of the beam under consideration. Note that the desired value of admittance increases with increasing frequency. However, the admittance of the *RL*-circuit decreases with increasing frequency. Consequently, the performance of the shunting network decays very rapidly as the excitation frequency deviates from the design frequency. This is an inherent disadvantage of the shunting circuit composed only of a resistor and an inductor even when its performance is improved by adopting the tuning method to minimize the modal response peaks, as in den Hartog's invariant point concept. To resolve this problem, an *RLC* circuit was considered to generate the increasing admittance with increasing frequency.

The values of R, L, and C were determined by matching the optimal admittance values (real and imaginary parts) and the first derivative of the imaginary part with respect to frequency at the tuning frequency. Matching the derivatives of the imaginary parts was necessary due to the strong dependence of performance on the reactance value. For the beam and the patch considered in this study, the values were determined as R=299 Ω, L=0.4460 H, and C=-0.1615 μF. A negative capacitance was required to achieve the desired variation of the admittance with frequency. The results are shown in Figure 10. The admittance follows the desired optimal values very closely near the tuning frequency. A negative capacitance could be implemented with an active filter such as a negative impedance converter. However, such a design would require an external power source.

C. Forced vibration of beam

To compare the capabilities of the various tuning criteria, the forced vibration response of a finite beam controlled by the shunts located at the clamped edge was considered. Figure 11 shows the forced vibration response calculated using the Rayleigh-Ritz method presented in section 4 for different values of elements in the *RLC* shunt circuit. When the admittance matches the optimal values over the entire frequency range, the modal response of the beam completely disappears and the beam response closely resembles that of an infinite beam. This suggests that the incident vibrational energy to the piezoelectric patch is completely absorbed and is dissipated into heat. When the *RLC* circuit employing negative capacitance is used to approximate the frequency dependent admittance, as in Figure 10, the performance is limited to a finite frequency range. The first (fundamental) modal response of the beam completely disappears. The shunting is also effective in reducing the response of the second and third modal response. At higher frequencies the damping capability rapidly decreases since the admittance deviates from the optimal values calculated here when the frequency increases from the design frequency. Compared to tuning methods based on the modal properties and den Hartog's invariant point concept, the current method based on the wave propagation approach is superior in regulating the forced vibration response of the beam.

6. CONCLUSIONS AND FUTURE WORK

The absorption and subsequent dissipation of structural vibration energy by piezoelectric patches was investigated. Dissipating converted electrical energy through piezoelectric effects into shunting electrical networks enhanced the damping of structural vibrations. Performance was strongly dependent on the parameters of the shunting elements. Optimization of these parameters was performed based on wave propagation characteristics, i.e., absorption, transmission, and reflection of bending waves propagating toward the piezoelectric patches attached to various locations of the beam. Following this approach, the modal properties of the beam were not considered in obtaining the optimal properties. The method applies to a broad range of frequencies and to frequency ranges affected by a large number of modes. The coupling between patches through modal response interaction of the beam can be neglected in the presented tuning method.

When a resistive shunting element was used, the vibration energy dissipation was maximum when the patch was attached to a clamped edge as opposed to the simply supported or free edge. When the patch was attached to the free edge, energy dissipation occurred only at high frequencies where the dimension of the patch was comparable to the wavelength of the propagating bending wave. The complete absorption of the incident vibration energy occurred when a resonant shunting network was used. The inherent disadvantage of using *RL* networks with frequency-independent resistance and inductance values was identified –the admittance of constant *RL* circuit decreases with increasing frequency while the calculated optimal admittance in this study increases with increasing frequency. Complete absorption was obtained at the design frequency when an *RLC* circuit with negative capacitance was employed. Implementation of a negative capacitance requires active filters such as a negative impedance converter. The *RLC* circuit designed according to wave propagation characteristics resulted in much better structural vibration control compared to conventional methods based on modal properties of the beam. Without requiring complicated control systems, such as feedback and feedforward controllers, the piezoelectric patches can achieve significantly improved performance by using a simple *RLC* circuit with appropriate tuning. Although, this technique was demonstrated here on a beam shunted with piezoelectric patch using *RL* or *RLC* electrical networks, the proposed numerical procedures can be applied to different electrical networks with minor modifications. Similar optimization procedures can be applied to a shunt patch attached to a plate by neglecting Poisson effects as for the optimization of the boundary stiffness of a viscoelastically-supported plate [18]. The experimental confirmation of the developed optimization method is in progress.

7. ACKNOWLEDGEMENTS

The first author gratefully acknowledges the financial support from the NASA Langley Research Center while in residence under a National Research Council Post-doctoral Research Associateship Award.

References

1. D. Zenkert *An Introduction to Sandwich Construction* (Chameleon Press Ltd., London, 1997).
2. A. Cummings, H.J. Rice, R. Wilson, "Radiation damping in plates, induced by porous media," J. Sound Vib. **221**, 143-167 (1999).
3. J.S. Bolton, N.M. Shiau, Y.J. Kang, "Sound transmission through multi-panel structures lined with elastic porous materials," J. Sound Vib. **191**, 317-347 (1996).
4. G.P. Gibbs, R.H. Cabell, D.L. Palumbo, R.J. Silcox, and T.L. Turner "Recent advances in active noise and vibration control at NASA Langley Research Center," J. Acoust. Soc. Am. **112**, 2346 (2002).

5. R.L. Forward, “Electronic damping of vibrations in optimal structures,” Appl. Optics. **18**, 690-697 (1979).
6. N.W. Hagood and A.von Flotow, “Damping of structural vibrations with piezoelectric materials and passive electrical networks,” J. Sound Vib. **146**, 243-268 (1991).
7. G.S. Agnes, “Development of a modal model for simultaneous active and passive piezoelectric vibration suppression,” J. Intel. Mat. Syst. Str. **191**, 317-347 (1996).
8. J.J. Hollkamp, “Multimodal passive vibration suppression with piezoelectric materials and resonant shunts,” J. Intel. Mat. Syst. Str. **191**, 317-347 (1996).
9. J. Tang and K.W. Wang, “Active-passive hybrid piezoelectric networks for vibration control: comparisons and improvement,” Smart Mater. Struct. **10**, 794-806 (2001).
10. M.B. Ozer and T.J. Royston, “Passively minimizing structural sound radiation using shunted piezoelectric materials,” J. Acous. Soc. Am. **114**, 1934-1946 (2003).
11. C.H. Park and D.J. Inman, “Enhanced piezoelectric shunt design,” Shock and Vibration. **10**, 127-133 (2003).
12. G. Caruso, “A critical analysis of electric shunt circuits employed in piezoelectric passive vibration damping,” Smart Mater. Struct. **10**, 1059-1068 (2001).
13. A.J. Fleming and S.O.R. Moheimani, “Adaptive piezoelectric shunt damping,” Smart Mater. Struct. **12**, 26-48 (2003).
14. C.H. Park, “Dynamics modeling of beams with shunted piezoelectric elements,” J. Sound Vib. **268**, 115-129 (2003).
15. C.L. Davis and G.A. Lesieutre, “Ac actively tuned solid state vibration absorber using capacitive shunting of piezoelectric stiffness,” J. Sound Vib. **232**, 601-617 (2000).
16. G.A. Lesieutre, “Vibration damping and control using shunted piezoelectric materials,” Shock Vib. Dig. **30**, 187-195 (1998).
17. B. Jaffe, R. Cook, and H. Jaffe, *Piezoelectric ceramics*, (Academic Press, New York, 1971).
18. J. Park, T. Siegmund, and L. Mongeau, “Influence of support properties on the forced vibrations of rectangular plates,” J. Sound Vib. **264**, 775-794 (2003).
19. A. Berry, J.-L. Guyader and J. Nicolas, “A general formulation for the sound radiation from rectangular, baffled plates with arbitrary boundary conditions,” J. Acous. Soc. Am. **88**, 2792-2802 (1990).
20. J. Park, T. Siegmund, and L. Mongeau, “Analysis of the flow-induced vibrations of viscoelastically supported rectangular plates,” J. Sound Vib. **261**, 225-245 (2003).

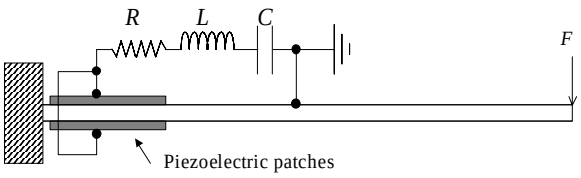

Figure 1. Shunted damping of flexural vibration using a piezoelectric patch.

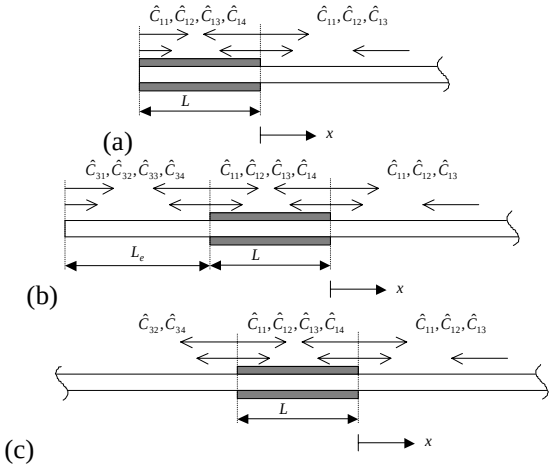

Figure 2. Wave propagation near the piezoelectric patch attached to different locations: (a) at edge, (b) near an edge, and (c) far from edges.

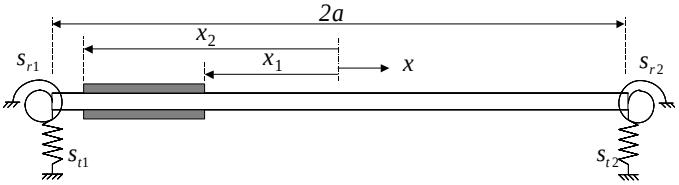

Figure 3. Flexural vibration of the beam under generally supported boundary condition.

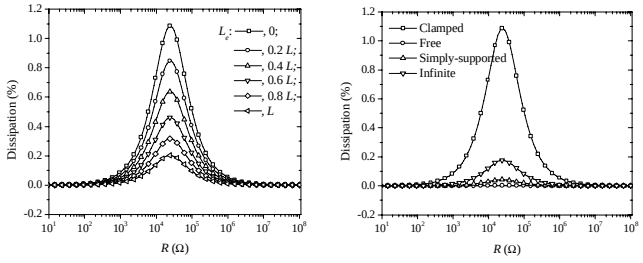

(a) (b)

Figure 4. Vibration energy dissipation of piezoelectric patches shunted by resistive networks. (a) Effect of separation distance from clamped edge, and (b) effects of several different boundary conditions.

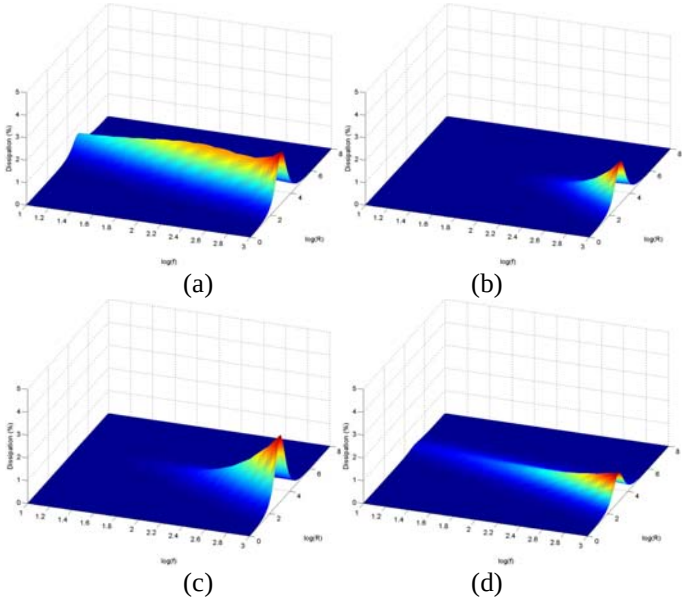

(a) (b) (c) (d)

Figure 5. Dissipation of incident vibration energy vs. frequency and resistance for resistive shunt and different boundary conditions at edges of beam: (a) clamped, (b) free, and (c) simply supported; and (d) far from both edges.

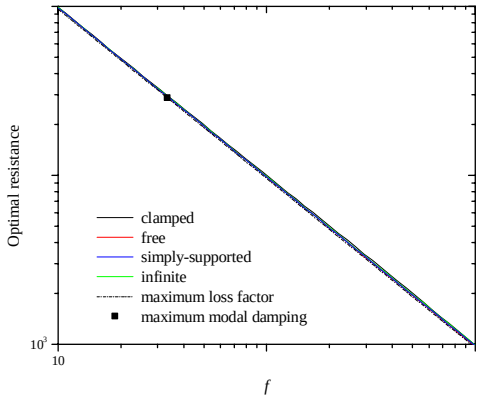

Figure 6. Optimal resistance calculated from two different tuning criteria: maximum dissipation of incident vibrational energy and maximum loss factor.

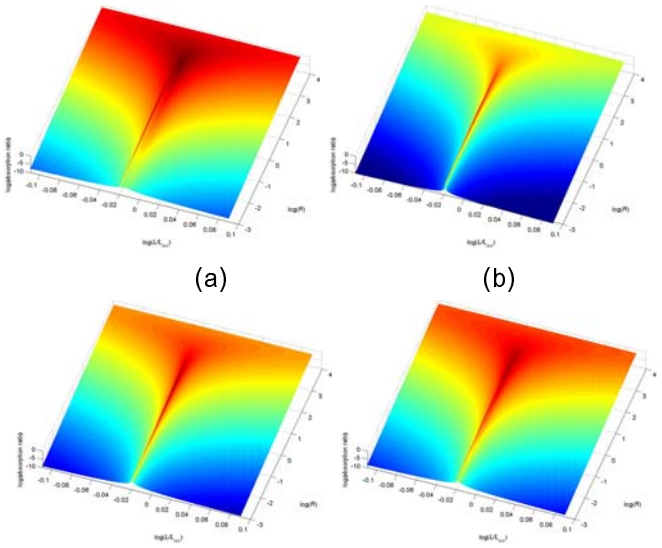

Figure 7. Dissipation of incident vibration energy vs. inductance and resistance for *RL* shunt and different boundary conditions at edges of beam: (a) clamped, (b) free, and (c) simply supported; and (d) far from both edges. f=33.5 Hz.

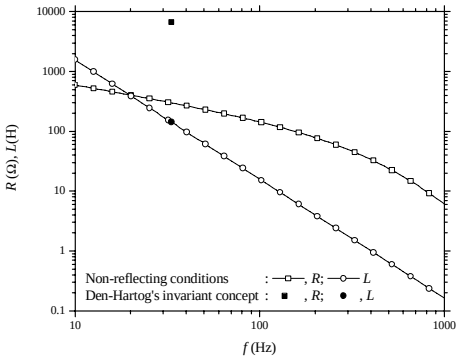

Figure 8. Optimal values of resistance and inductance to induce complete absorption of incident bending waves at piezoelectric patches attached to the clamped edge of the beam and its comparison to values calculated to minimize the modal response using den Hartog's invariant point concept [6].

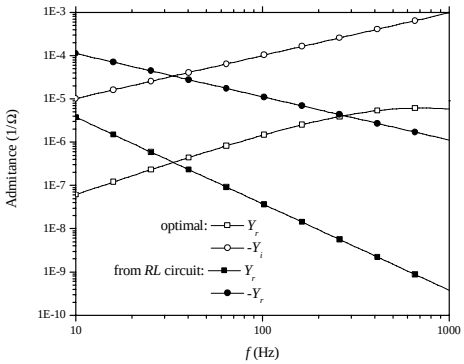

Figure 9. Optimal variation of the admittance to induce complete absorption of incident bending waves, and the admittance of the RL-circuit.

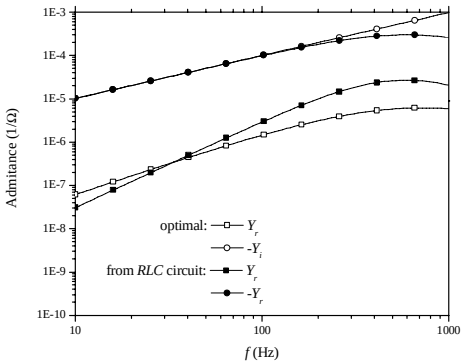

Figure 10. Optimal variation of the admittance to induce complete absorption of incident bending waves, and their approximation using *RLC* circuit (with negative capacitance).

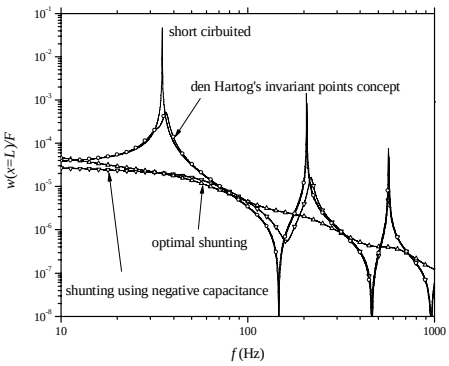

Figure 11. Damping of beam vibration using piezoelectric patches shunted by resonant shunting networks and comparison of different optimization criteria.